

# Lateral Diffusion of PEG-Lipid in Magnetically Aligned Bicelles Measured Using Stimulated Echo Pulsed Field Gradient $^1\text{H}$ NMR

Ronald Soong and Peter M. Macdonald

Department of Chemistry, University of Toronto, Ontario, Canada; and Department of Chemical and Physical Sciences, University of Toronto at Mississauga, Ontario, Canada

**ABSTRACT** Lateral diffusion measurements of PEG-lipid incorporated into magnetically aligned bicelles are demonstrated using stimulated echo (STE) pulsed field gradient (PFG) proton ( $^1\text{H}$ ) nuclear magnetic resonance (NMR) spectroscopy. Bicelles were composed of dimyristoyl phosphatidylcholine (DMPC) plus dihexanoyl phosphatidylcholine (DHPC) ( $q = \text{DMPC/DHPC}$  molar ratio = 4.5) plus 1 mol % (relative to DMPC) dimyristoyl phosphatidylethanolamine-*N*-[methoxy(polyethylene glycol)-2000] (DMPE-PEG 2000) at 25 wt % lipid.  $^1\text{H}$  NMR STE spectra of perpendicular aligned bicelles contained only resonances assigned to residual HDO and to overlapping contributions from a DMPE-PEG 2000 ethoxy headgroup plus DHPC choline methyl protons. Decay of the latter's STE intensity in the STE PFG  $^1\text{H}$  NMR experiment ( $g_z = 244 \text{ G cm}^{-1}$ ) yielded a DMPE-PEG 2000 (1 mol %, 35°C) lateral diffusion coefficient  $D = 1.35 \times 10^{-11} \text{ m}^2 \text{ s}^{-1}$ . Hence, below the “mushroom-to-brush” transition, DMPE-PEG 2000 lateral diffusion is dictated by its DMPE hydrophobic anchor.  $D$  was independent of the diffusion time, indicating unrestricted lateral diffusion over root mean-square diffusion distances of microns, supporting the “perforated lamellae” model of bicelle structure under these conditions. Overall, the results demonstrate the feasibility of lateral diffusion measurements in magnetically aligned bicelles using the STE PFG NMR technique.

## INTRODUCTION

Lateral diffusion of bilayer membrane components is fundamental to membrane function (for reviews, see Vaz et al., 1984; Jovin and Vaz, 1989; Tocanne et al., 1994; Almeida and Vaz, 1995; Saxton, 1999). Lateral diffusion coefficients vary by orders of magnitude: from the fast diffusion of small membrane-absorbed molecules such as anesthetics, to the slow diffusion of multi-helix or cytoskeleton-fixed transmembrane proteins.

Lateral diffusion of smaller species appears to follow a free volume model (Almeida et al., 1992a,b), whereas larger species appear to diffuse according to a hydrodynamic model (Saffman and Delbrück, 1975). For either diffusion regime, the presence of obstacles reduces the diffusion coefficient, and the details depend on the relative size and mobility of the diffuser versus the obstacle, and, especially, the area fraction of obstacles to diffusion. The latter can be problematic to estimate, particularly in cell membranes (Saxton, 1989). Moreover, the area fraction of obstacles in the transmembrane region can differ markedly from that in the extracellular region, since many membrane proteins have large extracellular domains attached to a single transmembrane helix.

Most lateral diffusion coefficients in membranes have been obtained using fluorescence recovery after photobleaching (FRAP) measurements of a fluorophore-tagged membrane-bound diffuser (Jovin and Vaz, 1989; Tocanne et al., 1994). Although FRAP is the most widely and

successfully employed technique for such measurements, the required attached fluorophore presents attendant synthetic challenges and concerns regarding perturbation, as well as limitations on measurement throughput. This suggests that it would be useful to have at hand alternate means of measuring membrane lateral diffusion coefficients, preferably in a rapid and nonperturbing fashion.

With this goal in mind, we undertook to examine the feasibility of pulsed field gradient (PFG) nuclear magnetic resonance (NMR) measurements of lipid lateral diffusion in bicelles.

NMR offers two basic means of measuring translational diffusion. One approach is to exploit the presence of an anisotropic interaction, such as the chemical shift, or dipolar, or quadrupolar interactions in anisotropic media, where the resonance frequency becomes a function of molecular orientation with respect to the magnetic field direction. Diffusion-mediated changes in molecular orientation then can be tracked using NMR exchange spectroscopy (EXSY) (Jeener et al., 1979). In lipid bilayer vesicles, specifically, lateral diffusion around the spherical vesicle's radius of curvature alters the molecular orientation relative to the magnetic field, thereby permitting lateral diffusion coefficients to be extracted from EXSY NMR data (Fenske and Jarrell, 1991). A complication is that the apparent diffusion coefficient measured by EXSY NMR is a convolution of the lateral diffusion coefficient and the vesicle's radius of curvature. Hence, two-dimensional  $^{31}\text{P}$  EXSY NMR measurements of phospholipid lateral diffusion coefficients have focused on phospholipid bilayers supported on spherical glass beads of known diameter (Picard et al., 1998).

Submitted April 6, 2004, and accepted for publication September 7, 2004.

Address reprint requests to Peter M. Macdonald, 3359 Mississauga Rd., Mississauga, ON L5L 1C6, Canada. Tel: 905-828-3805; Fax: 905-828-5425; E-mail: pmacdona@utm.utoronto.ca.

© 2005 by the Biophysical Society

0006-3495/05/01/255/14 \$2.00

doi: 10.1529/biophysj.104.043620

A second method is PFG NMR, in which a pulsed linear gradient of magnetic field is imposed across the sample such that the nuclear spin resonance frequency becomes transiently position-dependent (Stejskal and Tanner, 1965). The experiment is arranged such that refocusing of the nuclear spin magnetization in an echo-type experiment decreases with increasing translational diffusion in the direction of the applied field gradient. The PFG NMR method is well-established in studies of molecular diffusion in isotropic liquids (for reviews, see Stilbs, 1987; Kärger et al., 1988; Price, 1997, 1998), and can be applied to examine lateral diffusion in lipid bilayers macroscopically aligned in a magnetic field (Lindblom and Orädd, 1994; Orädd and Lindblom, 2004).

Two means of producing macroscopically aligned membranes are in common usage. One involves orienting the membranes between glass slides and placing the resulting "sandwiches" at the desired orientation (typically at the "magic" angle of  $54.7^\circ$  for lateral diffusion measurements) within the magnetic field of the NMR spectrometer (Lindblom and Orädd, 1994; Orädd and Lindblom, 2004). This same technology is employed to great advantage in studies of membrane protein structure via solid state NMR (Opella et al., 1999; Marassi, 2002).

Macroscopic alignment of lipid bilayers can also result when bicelles are placed in a magnetic field (for reviews, see Sanders et al., 1994; Sanders and Prosser, 1998). Bicelles, or bilayered micelles, are mixtures of long chain and short chain amphiphiles that self-assemble such that the long chain amphiphile forms a planar lipid bilayer, whereas the short chain amphiphile segregates to regions of high curvature at the edges of the bilayer. Sanders and Schwonek (1992) introduced the first bicelles composed entirely of phosphatidylcholines, mixing dimyristoyl phosphatidylcholine (DMPC) with dihexanoyl phosphatidylcholine (DHPC). When placed in a magnetic field, DMPC-rich bicelles spontaneously align such that the normal to the plane of the lipid bilayer is oriented perpendicular to the direction of the magnetic field (Ram and Prestegard, 1988). Alignment occurs only under the correct conditions of temperature, lipid concentration, and ratio of long/short chain lipids ( $q = \text{DMPC/DHPC}$ ) (Raffard et al., 2000). This property of magnetic alignment, along with their ease of preparation and high water content, suggest that bicelles are an ideal system in which to measure membrane lateral diffusion using PFG NMR techniques.

The morphology of bicelle structure remains, however, a point of continuing controversy. The classical picture, derived primarily from  $^{31}\text{P}$  NMR (Sanders and Prestegard, 1990) and knowledge of analogous systems (reviewed by Sanders et al., 1994), is that bicelles consist of discrete planar bilayer disks having DMPC sequestered to the planar bilayer disk body, with DHPC sequestered to the highly curved disk edges. Indeed, there is general agreement that this disk structure pertains at temperatures below the DMPC phase transition temperature and at low lipid concentrations and

low  $q$  ratios, where the bicelles are small and free to tumble isotropically. However, at higher lipid concentrations and/or higher  $q$  ratios, small-angle neutron scattering studies indicate a conversion to a morphology consisting of DMPC-rich continuous bilayer lamellae perforated by toroidal holes lined with DHPC (Nieh et al., 2001, 2002). This latter view is supported by the fluorescence resonance energy transfer studies of Rowe and Neal (2003), who argue further that discrete discoidal structures are inconsistent with the enormous viscosity increase observed under such conditions. The perforated lamellae morphology is also supported by the NMR diffusion studies of tetramethylsilane (TMS) sequestered within the bilayer interior as reported by Gaemers and Bax (2001). Nevertheless, freeze fracture electron micrograph images of bicelles quenched from higher temperature/higher  $q$ /higher lipid concentration solutions clearly contain discoidal structures (Arnold et al., 2002).  $^{31}\text{P}$  and  $^2\text{H}$  NMR spectroscopies are often used to generate phase diagrams for bicelle alignment (Arnold et al., 2002), since they readily differentiate powder distributions from magnetically aligned bicelles and isotropic phases. Furthermore, the spectral line shape reflects the quality of the magnetic alignment (Picard et al., 1999). On the other hand, such spectra do not differentiate readily between the disk and the perforated lamellae morphologies, since either morphology is consistent with the observed spectra. Neither does small-angle x-ray scattering (Bolze et al., 2000), given the difficulties of unique identification when too few reflections are observed (Lindblom and Rilfors, 1989). Hence, it would be useful to bring to bear other techniques capable of differentiating between the discoidal and the perforated lamellae models of bicellar morphology.

We describe here stimulated echo (STE) PFG  $^1\text{H}$  NMR measurements of the lateral diffusion coefficients of PEG-lipids incorporated into DMPC/DHPC bicelles aligned in the magnetic field of the NMR spectrometer. PEG-lipids consist of a hydrophobic anchoring group, such as dimyristoyl phosphatidylethanolamine (DMPE), to which a polyethyleneglycol (PEG) group is covalently attached through the lipid's polar headgroup. The water soluble PEG becomes effectively "grafted" to the lipid bilayer surface through its DMPE hydrophobic anchor. The resulting surface coating of PEG inhibits surface binding and adhesion via steric repulsion. Thus, PEG-coated lipid vesicles, known as "stealth" liposomes, are more effective drug delivery vehicles than vesicles lacking a PEG coating (Lasic and Needham, 1995). In bicelles, a surface coating of PEG is used to enhance bicelle stability, again by virtue of steric stabilization (King et al., 2000). The virtues of PEG-lipids as bio-compatibilizing agents have provoked intense research into their physicochemical properties, as reviewed recently by Marsh et al. (2003). To the best of our knowledge, however, no measurements of PEG-lipid lateral diffusion have been reported to date. As we demonstrate here, when incorporated into magnetically aligned bicelles, the

PEG-lipid's polyethylene glycol headgroup yields a narrow  $^1\text{H}$  NMR resonance that permits facile measurement of the PEG-lipid's lateral diffusion coefficient using STE PFG  $^1\text{H}$  NMR spectroscopy.

## EXPERIMENTAL

### Materials

DMPC (1,2-dimyristoyl-*sn*-glycero-3-phosphocholine), DHPC (1,2-dihexanoyl-*sn*-glycero-3-phosphocholine), and DMPE-PEG 2000 (1,2-dimyristoyl-*sn*-glycero-3-phosphoethanolamine-N-methoxy(polyethylene glycol)-2000) were purchased from Avanti Polar Lipids (Alabaster, AL). All other biochemicals and reagents were purchased from Sigma-Aldrich (Oakville, Canada).

### Sample preparation

Bicelles were prepared to consist of 25 wt % lipid in 75 wt % aqueous 150 mM NaCl + 50 mM Tris-HCl, pH 7.4, in  $\text{D}_2\text{O}$ , as described previously (Crowell and Macdonald, 1999; 2001). The ratio  $q$ , being the proportion of long/short chain amphiphiles (DMPC/DHPC), was kept constant at  $q = 4.5$ . The long chain amphiphiles were taken to include DMPC plus any added PEG-lipid, the latter expressed as a percentage of the former. All bicelle preparations were stored at  $4^\circ\text{C}$  before use. Magnetic alignment of the bicelles generally occurred within 30 min of the sample being placed in the field of the NMR spectrometer and warmed to  $35^\circ\text{C}$ , as assessed using  $^2\text{H}$  and  $^{31}\text{P}$  NMR spectroscopy.

### NMR spectroscopy

All NMR spectra were recorded on a Chemagnetics (Fort Collins, CO) CMX300 NMR spectrometer using a magnetic resonance imaging/spectroscopy probe (Doty Scientific, Columbia, SC) equipped with actively shielded gradient coils and dual radio frequency channels in addition to the lock channel. All spectra were recorded at a sample temperature of  $35^\circ\text{C} \pm 0.5^\circ\text{C}$ .

$^2\text{H}$  NMR spectra were recorded at 45.99 MHz using a single pulse on the lock channel with quadrature detection and complete phase cycling of the pulses. Typical acquisition parameters are as follows: a pulse length of  $100\ \mu\text{s}$  ( $90^\circ$ ), a recycle delay of 5 s, a spectral width of 5 kHz, and a 4 K data size. Spectra were processed with an exponential multiplication equivalent to 5 Hz line broadening before Fourier transformation, and were referenced to HDO.

$^{31}\text{P}$  NMR spectra were recorded at 121.6 MHz using a single pulse, quadrature detection, complete phase cycling of the pulses, and proton decoupling during the signal acquisition. Typical acquisition parameters are as follows: a  $90^\circ$  pulse length of  $20\ \mu\text{s}$ , a recycle delay of 3 s, a spectral width of 100 kHz, and a 4 K data size. Spectra were processed with an exponential multiplication equivalent to 50 Hz line broadening before Fourier transformation, and were referenced to 85% phosphoric acid.

$^1\text{H}$  NMR spectra were recorded at 299.6 MHz. Typical acquisition parameters are as follows: a  $90^\circ$  pulse length of  $50\ \mu\text{s}$ , a recycle delay of 5 s, a spectral width of 10 kHz, and a 4 K data size. Spectra were processed with an exponential multiplication equivalent to 5 Hz line broadening before Fourier transformation, and were referenced to tetramethylsilane. Proton  $T_1$  relaxation times were measured using a standard inversion recovery protocol, whereas  $T_2$  relaxation times were measured from the decay of the Hahn echo.

$^1\text{H}$  NMR diffusion measurements were performed using the PFG STE procedure (Tanner, 1970), with phase cycling of the radio frequency pulses to remove unwanted echoes (Fauth et al., 1986). The field gradient pulses were applied along the longitudinal ( $z$ ) direction exclusively. A train of three identical gradient pulses with a repetition period of  $\tau_1 + \tau_2$  was imposed

before the PFG STE sequence to equalize eddy current effects during the two transverse evolution periods (Gibbs and Johnson, 1991). At the gradient strengths employed here (typically  $244\ \text{G cm}^{-1}$ ), longitudinal eddy current induced distortions of either echo phase or amplitude were no longer apparent 5 ms after the gradient pulse, so that there was no advantage to employing the longitudinal eddy current delay sequence (Gibbs and Johnson, 1991). Gradient strength was calibrated from the known diffusion coefficient of HDO at  $25^\circ\text{C}$  (Mills, 1973).

## RESULTS

Fig. 1 shows  $^2\text{H}$  and  $^{31}\text{P}$  NMR spectra of magnetically aligned DMPC/DHPC ( $q = 4.5$ ) bicelles containing 1 mol % DMPE-PEG 2000, all obtained at  $35^\circ\text{C}$ . Panel A is a  $^2\text{H}$  NMR

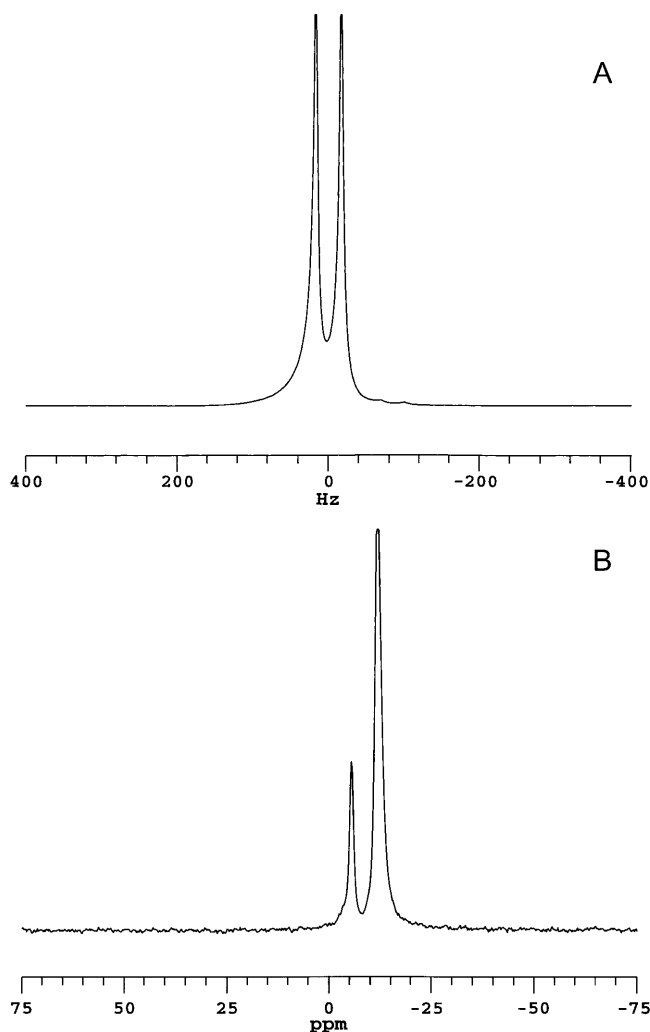


FIGURE 1 NMR spectra ( $35^\circ\text{C}$ ) of magnetically aligned bicelles: DMPC/DHPC ( $q = 4.5$ ) + 1 mol % DMPE-PEG 2000. (A)  $^2\text{H}$  NMR spectrum of HDO. The residual quadrupolar splitting of 30 Hz indicates magnetic alignment of bicelles. (B)  $^{31}\text{P}$  NMR spectrum showing resonances from DMPC ( $-12.4\ \text{ppm}$ ) and DHPC ( $-6.1\ \text{ppm}$ ), DMPC/DHPC intensity ratio of 4.5:1. The position of the DMPC resonance is indicative of bicelles aligned with their normal to the plane of the bilayer oriented perpendicular to the direction of the magnetic field. The resonance from 1 mol % DMPE-PEG 2000 is not resolved.

spectrum of HDO and exhibits a quadrupolar splitting equal here to 30 Hz, in agreement with previous reports (Ram and Prestegard, 1988; Losonczi and Prestegard, 1998; Ottinger and Bax, 1998). The residual quadrupolar splitting arises because HDO, being in fast exchange between free and aligned bicelle-surface-bound states, experiences a net isotropic motional averaging identically for all HDO molecules. In nonaligned bicelles, HDO exchanges between free water and bicelle-surface-bound water having either a broad distribution of orientations under high viscosity conditions, or an isotropic distribution of orientations under low viscosity conditions. In the latter case, the quadrupolar splitting collapses to zero. In the former, the  $^2\text{H}$  NMR spectrum of HDO broadens, reflecting the different net anisotropic motional averaging experienced by different HDO molecules. Hence the presence of a narrow residual quadrupolar doublet is diagnostic of a high degree of bicelle magnetic alignment.

Panel B in Fig. 1 is a  $^{31}\text{P}$  NMR spectrum of the same magnetically aligned bicelles and shows two narrow well-resolved resonances. The more intense upfield resonance occurs at  $-12.4$  ppm (referenced to 85%  $\text{H}_3\text{PO}_4$ ), the position expected for liquid-crystalline DMPC contained within a magnetically aligned bicelle oriented perpendicular to the direction of the magnetic field (Sanders et al., 1994). The second resonance occurs at  $-6.1$  ppm and has an integrated intensity of  $1/4.5$  relative to that at  $-12.4$  ppm, indicating that it arises from DHPC. The smaller residual chemical shift anisotropy of DHPC relative to DMPC is a consequence of the former's tendency to segregate into regions of high local curvature. The  $^{31}\text{P}$  NMR spectra confirm, therefore, that magnetic alignment of the bicelles has been achieved, and further indicate that the alignment of the bilayer normal is perpendicular to the magnetic field direction. The  $^{31}\text{P}$  NMR resonance due to 1 mol % DMPE-PEG 2000 is too small to discern in such spectra.

Fig. 2 shows a series of  $^1\text{H}$  NMR spectra of magnetically aligned DMPC/DHPC ( $q = 4.5$ ) bicelles containing increasing amounts of added DMPE-PEG 2000. Each spectrum was acquired using a spin echo pulse technique with an echo delay time of 10 ms. The bottom spectrum originated from magnetically aligned bicelles lacking any added DMPE-PEG 2000 and contains two well-resolved resonances: one at 4.2 ppm assigned to HDO, and another at 3.2 ppm assigned to the choline quaternary methyls of DHPC. With an echo delay time of 10 ms, the broad  $^1\text{H}$  NMR resonances expected from the acyl chain, glycerol backbone, or headgroup protons of DMPC (Finer et al., 1972; Cross et al., 1984), or any group experiencing significant residual homonuclear dipolar interactions, are not visible due to rapid transverse relaxation. The DHPC choline methyls experience a minimum of such interactions due to DHPC's preference for regions of high curvature within the bicelles.

The middle  $^1\text{H}$  NMR spectrum in Fig. 2 originated from magnetically aligned DMPC/DHPC ( $q = 4.5$ ) bicelles

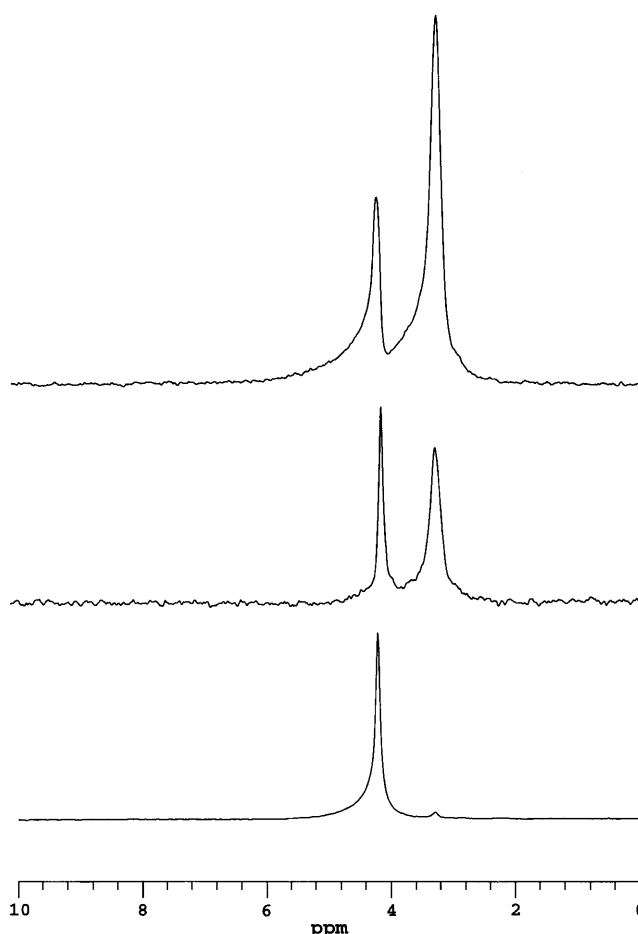


FIGURE 2  $^1\text{H}$  NMR spectra of magnetically aligned DMPC/DHPC ( $q = 4.5$ ) bicelles incorporating various amounts of DMPE-PEG 2000 and acquired using a spin echo sequence with a delay of 10 ms. The lower spectrum was obtained with bicelles lacking DMPE-PEG 2000. The intense resonance at 4.2 ppm is assigned to water, whereas the small resonance at 3.2 ppm is assigned to the choline quaternary methyls of DHPC. Other proton resonances are not visible due to their short transverse relaxation times. The middle spectrum was obtained with bicelles containing 1 mol % DMPE-PEG 2000. In addition to the water resonance, the ethoxy protons of the PEG group are readily visible at 3.3 ppm, overlapping the resonance of the DHPC choline quaternary methyls. The upper spectrum was obtained with bicelles containing 2 mol % DMPE-PEG 2000. The correspondence between the amount of DMPE-PEG 2000 and intensity of the resonance at 3.3 ppm is evident.

containing 1 mol % DMPE-PEG 2000. Again, two well-resolved resonances are observed. However, the relative intensity of the upfield resonance has increased and shifted slightly to 3.3 ppm. It is assigned, therefore, to a superposition of proton intensity at 3.3 ppm from the ethylene oxide units of the DMPE-PEG 2000 headgroup and the choline quaternary methyls of DHPC at 3.2 ppm. This interpretation is confirmed by the  $^1\text{H}$  NMR spectrum at the top that originated from magnetically aligned DMPC/DHPC ( $q = 4.5$ ) bicelles containing 2 mol % DMPE-PEG 2000, wherein the increase in the intensity of the resonance at 3.3 ppm is evident. However, it is equally evident that the intensity increase is not

simply proportional to the number of DMPE-PEG 2000 headgroup protons present. In fact, at 2 mol % DMPE-PEG 2000, the integrated intensity of the ethylene oxide proton resonance at 3.3 ppm is nearly 25% larger than expected relative to the case for 1 mol % DMPE-PEG 2000. This may be related back to differences in the dynamics of individual PEG ethylene oxide units as a function of their average distance from the bilayer surface (proximity to the surface being equated with relative immobilization), and the density distribution of ethylene oxide units relative to the surface changes with surface coverage of PEG-lipid. Further investigation would be required to more fully clarify this matter.

In summary, the  $^1\text{H}$  NMR spectrum of magnetically aligned DMPC/DHPC ( $q = 4.5$ ) bicelles containing DMPE-PEG 2000 and acquired using a Hahn spin echo technique with an echo delay on the order of 10 ms contains only two major resonances: one from residual HDO and the second from a superposition of DHPC choline methyl and DMPE-PEG 2000 ethylene oxide protons, the latter predominating. Other expected proton resonances are effectively invisible due to homonuclear dipolar broadening and their consequent rapid transverse relaxation. Overall, the  $^1\text{H}$  NMR spectra demonstrate that local segmental mobility within the PEG headgroup is quite high and virtually isotropic, despite being anchored to the bicelle through its attachment to DMPE. This enables the DMPE-PEG 2000 headgroup's  $^1\text{H}$  NMR resonance to be used in PFG NMR measurements of PEG-lipid center-of-mass lateral diffusion within the bicelle.

Fig. 3 illustrates the STE PFG NMR pulse sequence employed here for measurement of lateral diffusion coefficients (Tanner, 1970). In STE PFG NMR, the echo intensity decays with increasing strength of the applied gradient pulses according to Eq. 1,

$$I = I_0 \exp\left(\frac{-2\tau_2}{T_2}\right) \exp\left(\frac{-\tau_1}{T_1}\right) \exp(-\gamma^2 g^2 D \delta^2 [\Delta - \delta/3]), \quad (1)$$

where  $\gamma$  is the relevant magnetogyric ratio,  $g$  is the gradient pulse amplitude,  $D$  is the isotropic diffusion coefficient,  $\delta$  is the gradient pulse duration,  $\Delta$  is the experimental diffusion time, and  $T_1$  and  $T_2$  are the longitudinal and transverse relaxation times, respectively. Experimentally, either the gradient pulse amplitude, or its duration, or the diffusion time, is incremented progressively, and the diffusion coefficient is extracted from the slope in a plot of  $\ln(I/I_0)$  versus  $\gamma^2 g^2 \delta^2 (\Delta - \delta/3)$ . In the STE PFG NMR sequence,  $\Delta = \tau_1 + \tau_2$  so that for situations where  $T_1 > T_2$ , the experimentally accessible diffusion time is limited by  $T_1$  rather than  $T_2$ . The ability to employ longer diffusion times facilitates measurements for cases of slower diffusion, or lower gradient strengths, or lower  $\gamma$  nuclei.

For the case of anisotropic diffusion, pertinent to lipid lateral diffusion in membranes, the  $g^2 D$  term in Eq. 1 is replaced by  $\mathbf{g} \cdot \mathbf{D} \cdot \mathbf{g}$ , where  $\mathbf{D}$  is a symmetric Cartesian

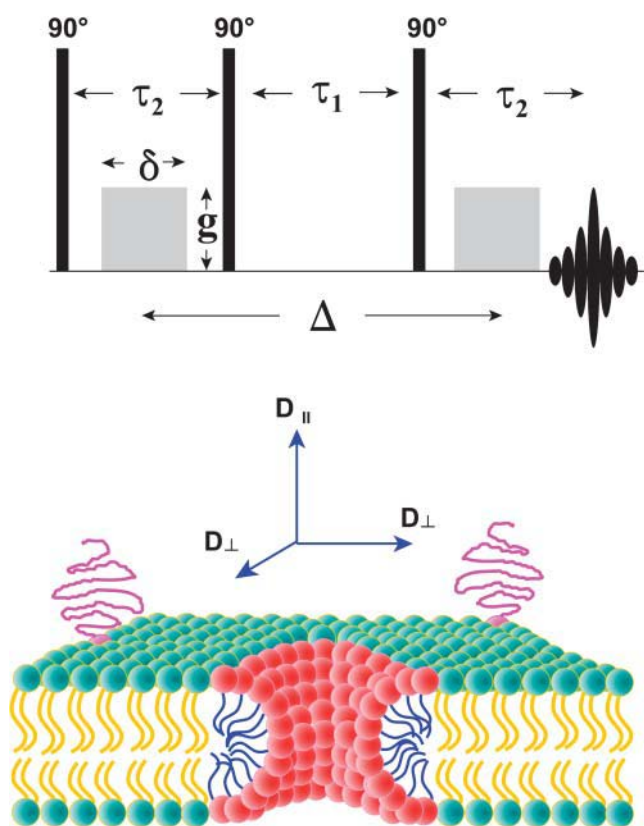


FIGURE 3 (Top) Stimulated echo (STE) pulsed field gradient (PFG) NMR sequence (Tanner, 1970). The phases of the three  $90^\circ$  radio frequency pulses and of the receiver are cycled to eliminate unwanted echoes (Fauth et al., 1986). During the first delay time  $\tau_2$ , a gradient pulse of amplitude  $g$  and duration  $\delta$  encodes the spins according to their position along the direction of the applied magnetic field gradient, in this case along the  $z$  direction. The spin magnetization is stored along the  $z$  direction during the second delay time  $\tau_1$  to take advantage of the case  $T_1 > T_2$ , thereby permitting longer diffusion times  $\Delta$ . During the third delay time  $\tau_2$ , the second gradient pulse decodes according to position along the direction of the applied gradient. The intensity of the stimulated echo that forms at a time  $\tau_2$  after the third radio frequency pulse decreases with increasing diffusion during the time as per Eq. 1. A train of three identical gradient pulses with a repetition period of  $\tau_1 + \tau_2$  was imposed before the STE PFG NMR sequence to equalize eddy current effects during the two transverse evolution periods (Gibbs and Johnson, 1991). (Bottom) Schematic cross section of a DMPC/DHPC bicelle in the perforated lamellae model morphology. DMPC (green-yellow) forms the lamellar bilayer region, whereas DHPC (red-blue) is sequestered into highly curved toroidal "holes" forming perforations in the lamellae. For amphiphiles resident within or upon the lamellar bilayer, such as the PEG-lipid (magenta) shown with its PEG headgroup extending into the aqueous bathing medium, the molecule-fixed diffusion tensor is completely described in terms of  $D_{\parallel}$  and  $D_{\perp}$ , referring to diffusion in a direction parallel or perpendicular, respectively, to the normal to the plane of the bilayer.  $D_{\perp}$  corresponds, therefore, to lateral diffusion within the plane of the bilayer.

diffusion tensor representing the diffusion process as defined in the laboratory frame (Stejskal and Tanner, 1965), and

$$\mathbf{g} \cdot \mathbf{D} \cdot \mathbf{g} = \sum_{\alpha} \sum_{\beta} D_{\alpha\beta} g_{\alpha} g_{\beta} \quad \alpha, \beta = x, y, z. \quad (2)$$

Thus, for field gradients applied solely along the laboratory,  $z$  direction  $\mathbf{g} \cdot \mathbf{D} \cdot \mathbf{g}$  becomes  $g_z^2 D_{zz}$ , and only the  $D_{zz}$  element of the diffusion tensor is measured. The diffusion tensor in the relevant molecular frame can be transformed into the laboratory frame in the usual way using rotation matrices. For a molecular frame defined with respect to the lipid bilayer, only two independent diffusion tensor elements persist: specifically,  $D_{\parallel}$  and  $D_{\perp}$  representing, respectively, diffusion parallel and perpendicular to the bilayer normal (Callaghan and Soderman, 1983; Lindblom and Orädd, 1994). This situation is illustrated schematically in Fig. 3 for the case of a bicelle, where it is clear that  $D_{\perp}$  corresponds to lateral diffusion within the bilayer. Hence, for the case of a field gradient applied parallel to the direction of the main magnetic field, the measured diffusion coefficient becomes,

$$D = D_{\perp} \sin^2 \theta + D_{\parallel} \cos^2 \theta, \quad (3)$$

where  $\theta$  is the polar angle between the bilayer normal and the magnetic field direction. It is reasonable to assume that diffusion parallel to the bilayer normal is many orders of magnitude slower than diffusion perpendicular to the bilayer normal, i.e., lateral diffusion, so the second term in Eq. 3 may be ignored. For spontaneously magnetically aligned bicelles, the bilayer normal is oriented at  $90^\circ$  relative to the magnetic field direction. Hence for a perfectly aligned bicelle sample, i.e., having an infinitely narrow mosaic spread of alignments, the apparent diffusion coefficient measured in our STE PFG NMR experiment is directly equal to the lateral diffusion coefficient within the bilayer.

For the case of well-resolved resonances, knowledge of  $T_1$  or  $T_2$  is not essential to diffusion coefficient measurements via the STE PFG NMR technique, since both  $\tau_1$  and  $\tau_2$  are constant in any one measurement series. For the case of overlapping or poorly resolved resonances, however, the echo intensity in the STE PFG NMR experiment is a sum of contributions, and knowledge of the individual  $T_1$  and  $T_2$  relaxation times is a prerequisite to extracting the individual diffusion coefficients from the overall intensity decay.

Table 1 lists values of  $T_1$  and  $T_2$  measured for the DMPE-PEG 2000 headgroup and the DHPC choline methyls in magnetically aligned bicelles at  $35^\circ\text{C}$ . The DHPC choline methyl  $T_1$  and  $T_2$  relaxation times were measured in magnetically aligned bicelles lacking PEG-lipid. In magnetically aligned bicelles containing PEG-lipid, where the DHPC choline methyl and PEG resonances overlap, their individual contributions to  $T_1$  inversion recovery intensities could not be resolved, and a weighted average value of  $T_1$  is reported.  $T_2$  spin echo intensities, on the other hand, were treated as a sum of DHPC choline methyl (short) plus PEG (long) contributions weighted according to their a priori relative intensities. This approach yielded somewhat better fits to the intensity data than using a single exponential fit. In all cases,  $T_1 > T_2$  by at least an order of magnitude,

**TABLE 1**  $^1\text{H}$  NMR longitudinal ( $T_1$ ) and transverse ( $T_2$ ) relaxation times for combined (DHPC choline methyl + DMPE-PEG 2000 headgroup) resonance in magnetically aligned bicelles

Bicelle composition	$X_{\text{DHPC}}^*$	$X_{\text{PEG}}^\dagger$	$T_1^\ddagger$ (ms)	$T_2^\S$ (ms)	
				Short	Long
DMPC/DHPC $q = 4.5$	1.0	0	485	18	—
+1% DMPE-PEG 2000	0.586	0.414	852	25	70
+2% DMPE-PEG 2000	0.414	0.586	827	20	60

\*Fractional contribution of the nine DHPC choline methyl protons given  $q = 4.5$ .

$^\dagger$ Fractional contribution of the DMPE-PEG 2000 headgroup protons based on four protons per 45 ethylene oxide units per DMPE-PEG 2000 at the indicated mole %.

$^\ddagger$ Intensities of the combined (DHPC choline methyls + DMPE-PEG 2000 headgroup) proton resonance in the inversion recovery experiment could not be resolved into separate contributions and were fit as a single exponential having the indicated  $T_1$ .

$^\S$ Intensities of the combined (DHPC choline methyls + DMPE-PEG 2000 headgroup) proton resonance in the spin echo experiment were fit to a double exponential weighted according to the a priori values of  $X_{\text{DHPC}}$  and  $X_{\text{PEG}}$  for the two contributing chemical groups. This approach gave somewhat better fits than using a single exponential.

indicating that the STE PFG NMR sequence is an optimal choice for diffusion measurements in these cases.

Fig. 4 shows a series of  $^1\text{H}$  NMR spectra of bicelles containing 1 mol % DMPE-PEG 2000 as a function of

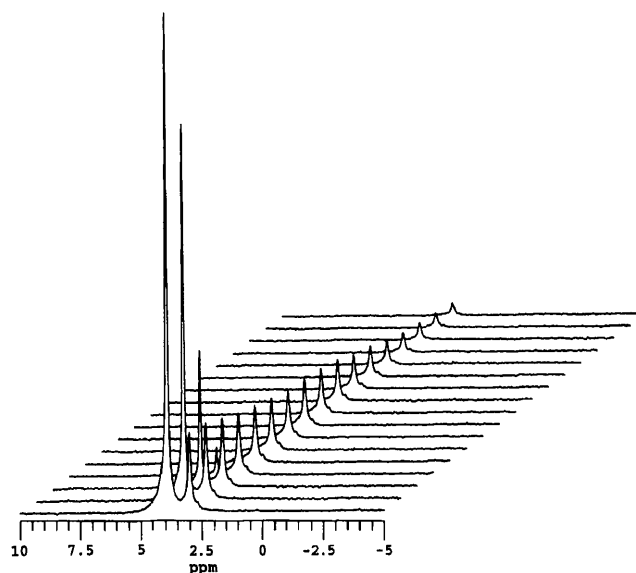


**FIGURE 4**  $^1\text{H}$  NMR spectra ( $35^\circ\text{C}$ ) of magnetically aligned DMPC/DHPC ( $q = 4.5$ ) + 1 mol % DMPE-PEG 2000 bicelles as a function of the field gradient pulse duration in the STE PFG NMR sequence. The gradient pulse amplitude was  $244 \text{ G cm}^{-1}$ , whereas  $\tau_2$  equaled 15 ms and  $\tau_1$  equaled 400 ms. Gradient pulse durations, from front to back in units of ms: 0.1, 0.25, 0.50, 0.75, 1.0, 1.25, 1.5, 1.75, 2.0, 2.5, 3.0, 3.5, 4.5, 5.5, 6.0, 6.5, and 7.0. The water resonance at 4.2 ppm decays rapidly due to water's fast diffusion. The combined DHPC choline methyl and DMPE-PEG 2000 headgroup resonance at 3.3 ppm decays far more slowly, as expected, for bilayer intercalated species.

increasing gradient pulse duration in the STE PFG NMR sequence. Here,  $\tau_1 = 400$  ms and  $\tau_2 = 15$  ms while the gradient strength was  $244 \text{ G cm}^{-1}$ . One notes that in every case, any broad background lipid resonances are absent due to their short  $T_2$  relative to  $\tau_2$ . The two remaining resonances are those of HDO and the combined (DHPC choline methyl + PEG headgroup) protons. The difference in their relative intensity versus the corresponding spectrum in Fig. 2 arises from the longer  $T_1$  and  $T_2$  relaxation times of HDO relative to those of the PEG headgroup protons and the differential effects this produces in the STE PFG NMR sequence. Of these two resonances, the HDO resonance intensity decays almost immediately to invisibility with increasing  $\delta$ , as anticipated, given water's rapid diffusion and the particular choices of gradient strength and delays  $\tau_1$  and  $\tau_2$ . The combined (DHPC choline methyl + PEG headgroup) resonance decays far more slowly, as expected for lipids constrained to diffuse laterally within a bicelle. Importantly, the particular choices of diffusion time  $\Delta = 415$  ms and gradient strength  $g = 244 \text{ G cm}^{-1}$  are sufficient to produce virtually complete decay of the resonance intensity over an accessible range of gradient pulse durations, which means that the lateral diffusion coefficient of the lipid can be measured reliably.

The diffusion coefficient is derived from a plot of  $\ln(I/I_0)$  versus  $\gamma^2 g^2 \delta^2 (\Delta - \delta/3)$  as shown in Fig. 5. For a population undergoing unrestricted center-of-mass diffusion characterized by a single uniform diffusion coefficient, such a plot

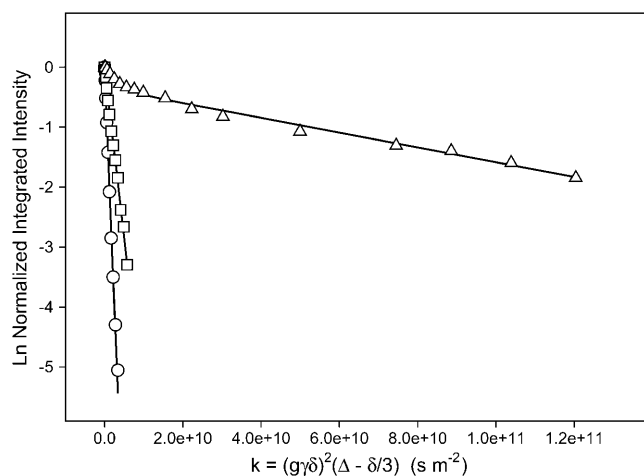


FIGURE 5 Normalized stimulated echo intensity decays from STE PFG  $^1\text{H}$  NMR spectra ( $35^\circ\text{C}$ ) of magnetically aligned DMPC/DHPC ( $q = 4.5$ ) bicelles  $\pm 1$  mole % DMPE-PEG 2000. Gradient amplitude =  $244 \text{ G cm}^{-1}$ . (○) Water,  $\Delta = 60$  ms,  $D_{\text{water}} = 1.6 \times 10^{-9} \text{ m}^2\text{s}^{-1}$ . (□) DHPC choline methyls in DMPC/DHPC ( $q = 4.5$ ) bicelles with no DMPE-PEG 2000,  $\Delta = 60$  ms,  $D_{\text{DHPC}} = 5.7 \times 10^{-10} \text{ m}^2\text{s}^{-1}$ . (△) Combined DHPC choline methyl + PEG headgroup protons in DMPC/DHPC ( $q = 4.5$ ) + 1 mol % DMPE-PEG 2000 bicelles,  $\Delta = 215$  ms,  $D_{\text{PEG}} = 1.35 \times 10^{-11} \text{ m}^2\text{s}^{-1}$ . The diffusion coefficients listed were obtained by fitting the experimental data to either Eq. 1 (water, DHPC) or Eq. 4, (PEG + DHPC) with values of the mole fractions  $X_{\text{DHPC}}$  and  $X_{\text{PEG}}$ , and  $T_1$  and  $T_2$  as per Table 1. Lines of best fit are shown.

should be linear with a slope proportional to the diffusion coefficient. Such is the case in Fig. 5 for the proton resonance of HDO in a magnetically aligned DMPC/DHPC  $q = 4.5$  bicelle sample at  $35^\circ\text{C}$  having a 75 wt % water content, where the water diffusion coefficient is measured to equal  $1.6 \times 10^{-9} \text{ m}^2\text{s}^{-1}$ . This is a factor of  $\sim 2$  slower water diffusion in bicelles relative to bulk water at the same temperature (Mills, 1973), the difference being attributed to the large fraction of bilayer surface-bound water in fast exchange with the bulk. Note that water diffusion in macroscopically oriented bilayers in general (Wästerby et al., 2002) and in magnetically aligned bicelles in particular (Chung and Prestegard, 1993; Gaemers and Bax, 2001) is anisotropic, with diffusion in the direction parallel to the bilayer normal considerably slower than in the perpendicular direction due to slow permeation of water across the bilayer.

The DHPC intensity decay shown in Fig. 5 was measured in magnetically aligned bicelles lacking DMPE-PEG 2000. The dependence on  $\delta$  is monoexponential and is fitted readily using a single diffusion coefficient equal to  $5.7 \times 10^{-10} \text{ m}^2\text{s}^{-1}$ . This represents diffusion comparable to that measured for DHPC micelles in solution (Andersson and Mäler, 2003) and is considerably faster than that measured for long-chain phosphatidylcholines confined to a lamellar bilayer (Tocanne et al., 1994), being a factor of  $\sim 50$  faster diffusion than that of DMPE-PEG 2000 discussed below. Moreover, the DHPC intensity decay indicates that DHPC diffusion is not restricted by confinement to either a discoidal or toroidal edge domain, but rather corresponds to diffusion distances on the order of tens of microns (see Eq. 6 in the Discussion). Several possible explanations for DHPC's relatively fast unrestricted diffusion present themselves. One is that DHPC is in fast exchange between bicelle-bound and free-in-solution or micellized populations. However, at the 25 wt % lipid content and  $q$  ratio employed here, the fraction of DHPC free in solution is expected to be exceedingly small (Sanders and Schwonek, 1992; Struppe and Vold, 1998). Alternately, DHPC may be in fast exchange between planar bilayer regions and regions of high local curvature within the bicelle, whether these are the edges of bicelle disks or of the toroids constituting the perforations in the perforated-lamellae model. Lipid lateral diffusion in the planar regions is dictated by free volume considerations (Almeida et al., 1992a,b), and a short chain species such as DHPC is expected to diffuse rapidly relative to a long-chain species like DMPC (Kuo and Wade, 1979). However,  $^{31}\text{P}$  NMR suggests that DMPC and DHPC remain highly segregated over a wide range of hydration levels, temperatures, and  $q$  values (Glover et al., 2001). Yet another explanation is that DHPC diffuses along a continuous path consisting of the edges of bicelle disks or toroids in close edge-to-edge contact. Further study will be required before a more definitive conclusion can be drawn. But one means of differentiating the various possibilities would be to examine the anisotropy of DHPC diffusion.

For the case of the combined (DHPC choline quaternary methyl + PEG headgroup) resonance, the integrated signal intensity in Fig. 5 is nonlinear, indicating the presence of multiple diffusion coefficients. If the diffusion can be characterized by a dispersion of diffusion coefficients about a single average value, then the signal attenuation can be fit using a stretched exponential (Nyström et al., 1993). However, this approach fails for the case of the combined (DHPC choline quaternary methyl + PEG headgroup) resonance. Instead, we find that the best description assumes only two diffusing species, one being DHPC and the other being DMPE-PEG 2000, according to Eq. 4,

$$\begin{aligned} I/I_0 = & X_{\text{DHPC}} \exp\left(\frac{-2\tau_2}{T_{2\text{DHPC}}}\right) \exp\left(\frac{-\tau_1}{T_{1\text{DHPC}}}\right) \exp(-kD_{\text{DHPC}}) \\ & + X_{\text{PEG}} \exp\left(\frac{-2\tau_2}{T_{2\text{PEG}}}\right) \exp\left(\frac{-\tau_1}{T_{1\text{PEG}}}\right) \exp(-kD_{\text{PEG}}), \quad (4) \end{aligned}$$

where  $k = (\gamma^2 g^2 \delta^2 (\Delta - \delta/3))$ , and  $X_{\text{DHPC}} = 1 - X_{\text{PEG}}$  is the fractional intensity contributed initially by the DHPC choline quaternary methyl protons, and  $D_{\text{DHPC}}$  and  $D_{\text{PEG}}$  are the diffusion coefficients of DHPC and DMPE-PEG 2000, respectively. Assuming that  $D_{\text{DHPC}}$  is unchanged by the presence of PEG-lipid, that all of both the DHPC choline quaternary methyl and the PEG headgroup protons are NMR visible, and employing the values of  $T_1$  and  $T_2$  for DHPC and DMPE-PEG 2000 listed in Table 1, the remaining unknown quantity,  $D_{\text{PEG}}$ , is obtained by fitting of the intensity decays as shown in Fig. 5.  $D_{\text{PEG}}$  is found to equal to  $1.35 \times 10^{-11} \text{ m}^2 \text{ s}^{-1}$ , which lies in the range expected for a diacyl phospholipid diffusing laterally within the plane of a liquid-crystalline lipid bilayer (Tocanne et al., 1994).

Fig. 6 A shows a series of STE PFG NMR intensity decays for the combined (DHPC choline quaternary methyl + DMPE-PEG 2000 headgroup) resonance for different values of the diffusion time  $\Delta = \tau_1 + \tau_2$ , in which  $\tau_2$  was held constant at 15 ms, whereas  $\tau_1$  was altered progressively from 200 to 400 to 600 ms. The intensity decay is progressively greater with increasing  $\Delta$  due to the combined effects of  $T_1$  relaxation and longer diffusion time. In each instance, the intensity decay is apparently biexponential. The curves of best fit shown in the figure were obtained using Eq. 4 employing the known values of  $X_{\text{PEG}}$  and  $X_{\text{DHPC}}$ , constant values of  $T_1$  and  $T_2$  for the DHPC choline methyl, and the DMPE-PEG 2000 headgroup protons as per Table 1, allowing  $D_{\text{DHPC}}$  to equal  $5.7 \times 10^{-10} \text{ m}^2 \text{ s}^{-1}$  as measured in bicelles lacking PEG-lipid, and inputting  $D_{\text{PEG}}$  as the parameter of fit for the three different diffusion times. The success of this approach is evident. It is found that for all three diffusion times,  $D_{\text{PEG}} = 1.35 \times 10^{-11} \text{ m}^2 \text{ s}^{-1}$  at 1 mol % DMPE-PEG 2000, a value similar to the diffusion coefficient measured via FRAP for liquid-crystalline DMPC (Tocanne et al., 1994).

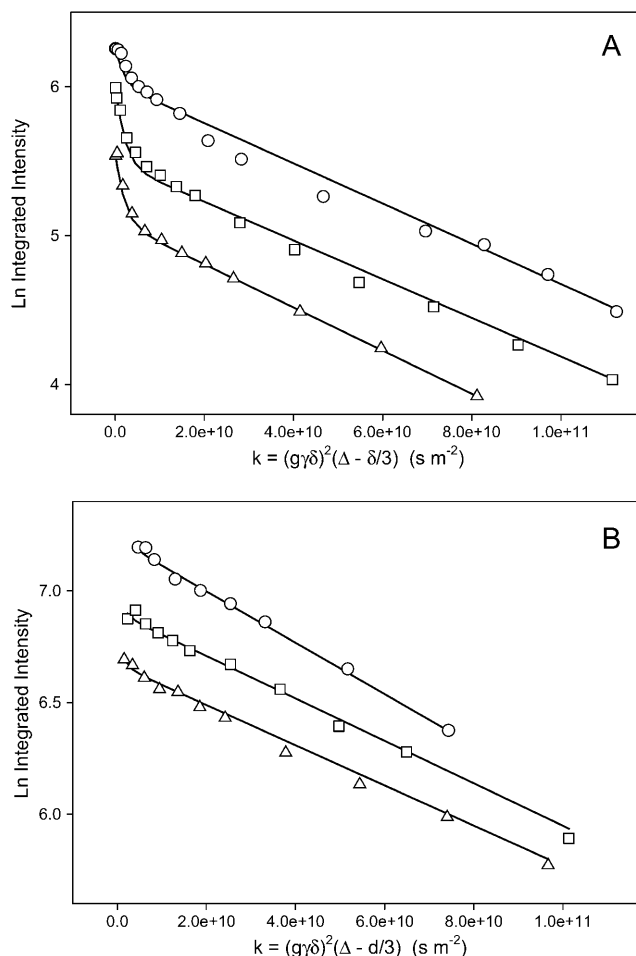


FIGURE 6 (A) Stimulated echo intensity decays for different diffusion times in STE PFG  $^1\text{H}$  NMR spectra (35°C) of magnetically aligned DMPC/DHPC ( $q = 4.5$ ) bicelles + 1 mol % DMPE-PEG 2000. Gradient amplitude  $244 \text{ G cm}^{-1}$ . ( $\circ$ )  $\Delta = 215 \text{ ms}$ , ( $\square$ )  $\Delta = 415 \text{ ms}$ , ( $\triangle$ )  $\Delta = 615 \text{ ms}$ . Lines of best fit using Eq. 4 are shown with  $D_{\text{DHPC}} = 5.7 \times 10^{-10} \text{ m}^2 \text{ s}^{-1}$ ,  $D_{\text{PEG}} = 1.35 \times 10^{-11} \text{ m}^2 \text{ s}^{-1}$ , and values of  $X_{\text{DHPC}}$ ,  $X_{\text{PEG}}$ ,  $T_1$ , and  $T_2$  as per Table 1. (B) Stimulated echo intensity decays for different diffusion times in STE PFG  $^1\text{H}$  NMR spectra (35°C) of magnetically aligned DMPC/Na glycocholate ( $q = 4.5$ ) bicelles + 1 mol % DMPE-PEG 2000. Gradient amplitude  $244 \text{ G cm}^{-1}$ . Lines of best fit using Eq. 1 are shown. ( $\circ$ )  $\Delta = 215 \text{ ms}$ ,  $D_{\text{PEG}} = 1.10 \times 10^{-11} \text{ m}^2 \text{ s}^{-1}$ . ( $\square$ )  $\Delta = 415 \text{ ms}$ ,  $D_{\text{PEG}} = 0.95 \times 10^{-11} \text{ m}^2 \text{ s}^{-1}$ . ( $\triangle$ )  $\Delta = 615 \text{ ms}$ ,  $D_{\text{PEG}} = 0.90 \times 10^{-11} \text{ m}^2 \text{ s}^{-1}$ .

There are several alternate explanations conceivable for the biexponential decays of the combined (DHPC choline methyl + DMPE-PEG 2000 headgroup) resonance in the STE PFG  $^1\text{H}$  NMR experiment shown in Fig. 6 A. In particular, it may be the case that, rather than a combination of DHPC choline methyl plus DMPE-PEG 2000 intensity decay, one is instead observing, solely, or largely, the effects of some chemical and/or physical heterogeneity of the DMPE-PEG 2000. To confirm our original interpretation, we constructed bicelles in which DHPC was replaced by sodium glycocholate, an anionic bile salt shown by

Ram and Prestegard (1988) to form magnetically alignable self-assemblies. Sodium glycocholate was chosen in preference to CHAPSO, another bile salt used to produce magnetically aligned bicelles (Sanders et al., 1994), because the latter contains quaternary methyls giving rise to a  $^1\text{H}$  NMR resonance at 3.2 ppm (Meyerhoffer et al., 1992), whereas the former does not (Mukidjam et al., 1986). In our hands, mixtures of  $q = 4.5$  (DMPC/sodium glycocholate) plus 1 mol % DMPE-PEG 2000, 25 wt % lipid content, aligned readily in our magnetic field using the procedure described by Ram and Prestegard (1988). Specifically, at 35°C, the residual quadrupole splitting in the  $^2\text{H}$  NMR spectrum of HDO equaled 40 Hz, whereas the  $^{31}\text{P}$  NMR spectrum consisted of a single resonance at a frequency of  $-12.4$  ppm, indicating that these assemblies aligned well with the normal to the plane of the bilayer oriented perpendicular to the direction of the magnetic field (data not shown).

$^1\text{H}$  NMR spectra of glycocholate-containing bicelles in the absence of DMPE-PEG 2000 exhibited no resonance in the vicinity of 3.3 ppm. In the presence of DMPE-PEG 2000, the spectra consisted, again, of two resonances: one assigned to HDO and the other to the PEG protons as previously. Fig. 6 *B* shows the intensity decay of the PEG resonance in the STE PFG  $^1\text{H}$  NMR experiment as a function of the gradient pulse duration for three different diffusion times  $\Delta$ . It is apparent that these intensity decays are now monoexponential. This result confirms the original interpretation of the biexponential decays seen in Fig. 6 *A* as arising from a superposition of the DHPC plus DMPE-PEG 2000 decays. As was found with DHPC-containing bicelles, the measured DMPE-PEG 2000 diffusion coefficient is virtually independent of the experimental diffusion time, although the diffusion is somewhat slower due to the higher viscosity of the glycocholate-containing bicelles preparations.

Fig. 7 compares the STE PFG NMR intensity decays for magnetically aligned DMPC/DHPC ( $q = 4.5$ ) bicelles for the cases of 1 mol % and 2 mol % DMPE-PEG 2000. The DHPC diffusion coefficient derived by fitting the intensity decays as described above is identical in both cases. The DMPE-PEG 2000 diffusion coefficient, however, decreases from  $1.35 \times 10^{-11} \text{ m}^2\text{s}^{-1}$  at 1 mol % to  $1.15 \times 10^{-11} \text{ m}^2\text{s}^{-1}$  at 2 mol % DMPE-PEG 2000. Since the uncertainty in the measured diffusion coefficients is on the order of  $\pm 5\%$ , this difference appears to be significant. At both concentrations, the diffusion of the DMPE-PEG 2000 could be described in terms of a single diffusion coefficient having a narrow dispersion, as evident from the linearity of the portion of the intensity decay attributable to DMPE-PEG 2000. Also shown in the figure are intensity decays for the identical amounts of nonhydrophobically-modified PEG 2000 present in the interstices between bicelles. The diffusion coefficients fall in the range  $5.23 \times 10^{-10} \text{ m}^2\text{s}^{-1}$ . Clearly, the DMPE-PEG 2000 diffusion is limited by the diffusion of its hydrophobic anchor rather than by its extramembranous domain.

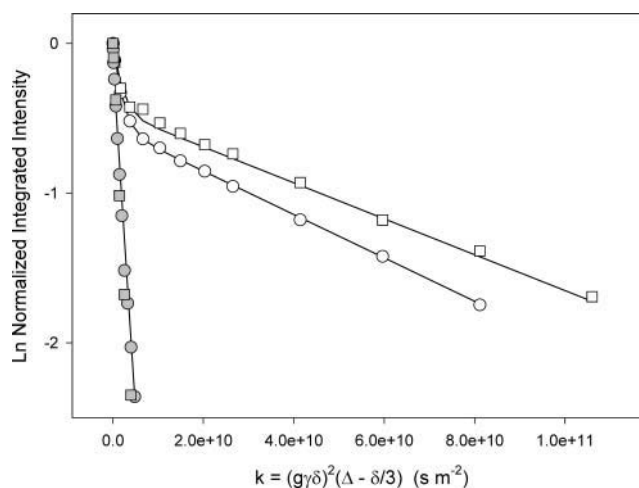


FIGURE 7 Stimulated echo intensity decays as a function of DMPE-PEG 2000 concentration in STE PFG  $^1\text{H}$  NMR spectra (35°C) of magnetically aligned DMPC/DHPC ( $q = 4.5$ ) bicelles plus various levels of either DMPE-PEG 2000 or free (i.e., nonhydrophobically modified) PEG 2000. Gradient amplitude  $244 \text{ G cm}^{-1}$ . (Open circles) 1 mol % DMPE-PEG 2000,  $\Delta = 615 \text{ ms}$ ,  $D_{\text{PEG}} = 1.35 \times 10^{-11} \text{ m}^2\text{s}^{-1}$ . (Open squares) 2 mol % DMPE-PEG 2000,  $\Delta = 615 \text{ ms}$ ,  $D_{\text{PEG}} = 1.15 \times 10^{-11} \text{ m}^2\text{s}^{-1}$ . (Shaded circles) 1 mol % free PEG 2000,  $\Delta = 60 \text{ ms}$ ,  $D_{\text{PEG}} = 5.00 \times 10^{-10} \text{ m}^2\text{s}^{-1}$ . (Shaded squares) 2 mol % free PEG 2000,  $\Delta = 60 \text{ ms}$ ,  $D_{\text{PEG}} = 5.23 \times 10^{-10} \text{ m}^2\text{s}^{-1}$ . DMPE-PEG 2000 diffusion coefficients were obtained using Eq. 4, the appropriate values of  $X_{\text{DHPC}}$ ,  $X_{\text{PEG}}$ , and the relaxation times in Table 1. Free PEG 2000 diffusion coefficients were obtained using Eq. 1.

## DISCUSSION

Previous PFG NMR diffusion studies in bicelles have focused primarily on small molecule tracer diffusion to characterize bicelle morphology. For example, Chung and Prestegard (1993) examined the anisotropy of water diffusion and concluded that it was consistent with a discoidal bicelle morphology. Gaemers and Bax (2001) examined the anisotropy of water and threonine diffusion to probe the aqueous medium, and TMS diffusion to probe the lipidic medium, in DMPC/DHPC ( $q = 3.2$ ) bicelles. They concluded that the distance over which TMS was observed to diffuse in magnetically aligned bicelles was consistent with a perforated lamellar bilayer morphology. In a different type of study, Andersson and Mäler (2003) used PFG NMR diffusion measurements in isotropic  $q = 0.5$  bicelles to probe interactions of the peptide motilin with lipid bilayers. Under their conditions, isotropic translational diffusion of entire bicelles occurs, and an increase in bicelle diffusion upon motilin binding was observed, presumably reflecting a decrease in bicelle size.

The results presented in this report are, to the best of our knowledge, the first to demonstrate the ability to measure lateral diffusion of amphiphiles in lipid bilayers using PFG NMR techniques and magnetically aligned bicelles as a model membrane system. Table 2 summarizes the values of the lateral diffusion coefficients obtained using STE PFG

**TABLE 2 STE PFG  $^1\text{H}$  NMR lateral diffusion coefficients for DHPC choline methyl and DMPE-PEG 2000 in magnetically aligned bicelles**

Bicelle composition	$X_{\text{DHPC}}^*$	$X_{\text{PEG}}^\dagger$	Diffusion coefficient ( $\text{m}^2\text{s}^{-1}$ )	
			DHPC	DMPE-PEG 2000
DMPC/DHPC $q = 4.5$	1.0	0	$5.7 \times 10^{-10}$	—
+1% DMPE-PEG 2000	0.586	0.414	$5.7 \times 10^{-10}$	$1.35 \times 10^{-11}$
+2% DMPE-PEG 2000	0.414	0.586	$5.7 \times 10^{-10}$	$1.15 \times 10^{-11}$

\*Fractional contribution of the nine DHPC choline methyl protons given  $q = 4.5$ .

$^\dagger$ Fractional contribution of the DMPE-PEG 2000 headgroup protons based on four protons per 45 ethylene oxide units per DMPE-PEG 2000 at the indicated mole %.

$^1\text{H}$  NMR in this fashion for DHPC and DMPE-PEG 2000 in the various situations investigated. In the following, we first discuss those aspects of the results pertaining specifically to PEG-lipids. We then address the general question of the prospects for employing this method of lateral diffusion measurement for other membrane-associating species using other NMR-sensitive nuclei.

### PEG-lipid diffusion in bicelles

Theory and experiment indicate that in bilayer membranes, when the size of the diffusing species is on the order of the “fluid” through which it is diffusing, in this case the bilayer lipids themselves, diffusion conforms to a free-volume model, whereas larger species follow a continuum hydrodynamic model (Saffman and Delbrück, 1975; Vaz et al., 1982; 1985; Tamm, 1991; Johnson et al., 1996). The critical dimension is the surface area occupied by the diffusing species. The crossover between the free volume and the hydrodynamic regimes occurs at surface areas as low as  $1 \text{ nm}^2$  (Liu et al., 1997). More subtly, the “triple layer” model of Liu et al. (1997) divides the membrane into a central, relatively low viscosity region separating two surface-interface regions of relatively high viscosity. Molecules exclusively occupying the central region are supposed to diffuse faster than the lipids; those spanning one-half the bilayer have their diffusion limited by the high viscosity surface region, whereas those spanning the entire bilayer are doubly limited by their presence in both high viscosity regions. A particular prediction arising from this scenario is that the size of any extramembranous portion of the diffusing species is largely irrelevant, because the water bathing the membrane is the least viscous zone relative to the membrane proper. Thus, lipid anchored proteins, for example, are predicted to have lateral diffusion coefficients similar to the lipids themselves.

This prediction is confirmed for the case of DMPE-PEG 2000, where the lateral diffusion coefficient of  $D = 1.35 \times 10^{-11} \text{ m}^2\text{s}^{-1}$  for 1 mol % DMPE-PEG 2000 in  $q = 4.5$  DMPC/DHPC bicelles at  $35^\circ\text{C}$  agrees with values reported

for DMPC using FRAP (Tocanne et al., 1994). Thus, the hydrophobic DMPE attachment anchoring the PEG group to the lipid bilayer is the primary determinant of the rate of lateral diffusion of PEG-lipid. Nonhydrophobically anchored PEG 2000 diffusing between bicelles, in contrast, diffuses an order of magnitude faster.

The observation that lateral diffusion is slower when the DMPE-PEG 2000 concentration is increased from 1 mol % to 2 mol % demonstrates that interactions between PEG-lipids exert at least some influence, albeit secondary, on lateral diffusion. At the DMPE-PEG 2000 concentrations employed here, the most likely PEG-PEG interactions are intralamellar, i.e., between PEG-lipids located on the same monolayer. This conclusion follows from a consideration of the size of the extramembranous PEG group relative to the available space. At concentrations well below some critical “overlap” concentration, PEG-PEG interactions are rare, and the shape of the hydrophobically anchored PEG group is modeled as a half-sphere or “mushroom” extending out from the surface a distance  $R_F$  and covering an area  $A = \pi R_F^2$  (de Gennes, 1980). The radius,  $R_F$ , of such an unperturbed surface-anchored random polymer chain in a good solvent is calculated according to the Flory equation (Flory, 1971),

$$R_F = N^{3/5}a, \quad (5)$$

where  $N$  is the degree of polymerization, i.e., the number of monomers, and  $a$  is the length of one monomer, taken to equal  $3.5 \text{ \AA}$  in the case of PEG (Hristova and Needham, 1995). For DMPE-PEG 2000, with 45 ethylene oxide units, the calculation yields a Flory radius of  $R_F \approx 35 \text{ \AA}$ . This is far less than the interlamellar spacing of  $\sim 136 \text{ \AA}$  that one calculates for liquid-crystalline DMPC lamellae at 25 wt % DMPC in water, assuming a DMPC monolayer thickness of  $20 \text{ \AA}$ . Thus, interlamellar PEG-PEG interactions are likely to be minimal. On the other hand, intralamellar PEG-PEG interactions are likely to be profound. Specifically, for DMPE-PEG 2000 in a DMPC bilayer, assuming DMPC occupies a footprint of  $60 \text{ \AA}^2$ , complete coverage of the bilayer is achieved at  $\sim 1.7 \text{ mol \%}$  (Du et al., 1997). Thus, increasing the DMPE-PEG 2000 concentration from 1 mol % to 2 mol % forces the PEG groups to begin to overlap and entangle, with slower lateral diffusion being a direct consequence of such intralamellar interactions. The PEG groups are not hard obstacles, however. Rather, as the surface density increases, the PEG groups can undergo a “mushroom-to-brush” transition involving a shape shift to a more extended conformation. Thus, even at 2 mol % DMPE-PEG 2000, where the surface coverage with PEG is ostensibly complete, lateral diffusion remains rapid.

The intensity decays in Figs. 6 and 7 at longer values of  $\delta$  are dominated by  $D_{\text{PEG}}$ , since the PEG-lipid diffuses more slowly than DHPC by a factor of  $\sim 50$ . Within the limits of accuracy of the data, the intensity decays in this region appear linear. Moreover, the diffusion coefficient extracted

from such decays is independent of the particular diffusion time  $\Delta$ . Hence, diffusion of the PEG-lipid can be described in terms of a single narrow-dispersion diffusion coefficient, uncomplicated by considerations of restricted or anomalous diffusion. The implication is that the PEG-lipid diffuses freely over a root mean-square distance,

$$\langle r^2 \rangle^{1/2} = [4Dt]^{1/2}, \quad (6)$$

where  $D$  is the diffusion coefficient and  $t = \Delta$  is the characteristic experimental diffusion time. For  $D = 1.35 \times 10^{-11} \text{ m}^2\text{s}^{-1}$  and  $\Delta = 615 \text{ ms}$ , the root mean-square diffusion distance of DMPE-PEG 2000 equals  $5.76 \text{ }\mu\text{m}$ . This far exceeds the  $300 \text{ }\text{\AA}$  radius of an “ideal” discoidal bicelle calculated as per Vold and Prosser (1996) for the case  $q = 4.5$  and tends, therefore, to support the perforated lamellae model of bicelle structure under these conditions (Nieh et al., 2001, 2002). A similar conclusion was reached by Gaemers and Bax (2001) from their examination of TMS diffusion in bicelles.

There are several problematic aspects of PFG NMR lateral diffusion measurements in bicelles that have not yet been mentioned. One is the potential contribution of “whole bicelle” translational diffusion to the apparent lateral lipid diffusion. Indeed, Andersson and Mäler (2003) exploited changes in the diffusion of isotropic  $q = 0.5$  bicelles to probe binding of the peptide motilin. However, for the bicelle solutions employed in our measurements, translational diffusion of “whole bicelles” is expected to be orders of magnitude slower than lateral lipid diffusion. Specifically, under our conditions ( $q = 4.5$ , 25 wt % lipid and  $35^\circ\text{C}$ ), the solution viscosity is extremely high, in agreement with the report of Struppe and Vold (1998) on comparable bicelles, where viscosity increases of up to 3 orders of magnitude were found. Assuming a discoidal bicelle of radius  $300 \text{ }\text{\AA}$ , as derived from the expression of Vold and Prosser (1996) for  $q = 4.5$ , the Stokes-Einstein equation yields a “whole bicelle” diffusion coefficient of  $7 \times 10^{-15} \text{ m}^2\text{s}^{-1}$  if the viscosity is 1000-fold that of water. Given that this is orders of magnitude slower diffusion than lateral diffusion within the bicelles, one may safely conclude that translational diffusion of entire bicelles makes no significant contribution to the measured lateral diffusion coefficients.

The quality of the alignment of the bicelles with respect to the magnetic field direction, however, will have a profound influence on the apparent lateral diffusion coefficient. Specifically, Eq. 3 demonstrates that the apparent lateral diffusion coefficient measured in the laboratory frame is scaled according to the angle between the bilayer normal and the magnetic field direction. In magnetically aligned bicelle solutions, both static and dynamic deviations from the ideal  $\theta = 90^\circ$  orientation can occur. Any static distribution of bicelle orientations is revealed in the  $^{31}\text{P}$  NMR spectrum of the phospholipids, as discussed by Picard et al. (1999) and Arnold et al. (2002). For the magnetically aligned bicelles employed

in our studies, the  $^{31}\text{P}$  NMR spectra (e.g., Fig. 1) exhibit line shapes and widths consistent with a highly uniform, narrow mosaic spread of alignment across all bicelles in the sample. The discussion highlights, however, the necessity of assessing the quality of bicelle alignment in each case.

Dynamic deviations from the ideal alignment can arise due to bicelle “wobble” about the average orientation. As proposed by Sanders and Schwonek (1992), the extent of bicelle wobble is assessed by calculating an order parameter,  $0 \leq S_{\text{bilayer}} \leq 1$ , intended to account for collective motions of the bicelles occurring in excess of those molecular motions common to lipid bilayers otherwise. For perpendicular aligned bicelles,  $S_{\text{bilayer}}$  may be obtained by comparing the residual anisotropic chemical shift of the DMPC  $^{31}\text{P}$  NMR resonance in bicelles with that of DMPC in multilamellar vesicles as per Eq. 7,

$$S_{\text{bilayer}} = (\delta_{\text{obs}} - \delta_{\text{iso}}) / (\delta_{90\text{MLV}} - \delta_{\text{iso}}), \quad (7)$$

where  $\delta_{\text{obs}}$  is the observed chemical shift position relative to the isotropic average chemical shift  $\delta_{\text{iso}}$ , whereas  $\delta_{90\text{MLV}}$  is the chemical shift of the high field shoulder in the  $^{31}\text{P}$  NMR spectrum of a multilamellar vesicle dispersion of DMPC at the same temperature. Sanders and Schwonek (1992) found  $S_{\text{bilayer}}$  approached 1.0 as  $q$  increased above 5, and approached zero as  $q$  decreased below  $\sim 2$ . In our case, with  $q = 4.5$ , we find  $S_{\text{bilayer}} \approx 0.85$ , in agreement with others (Sanders and Schwonek, 1992; Raffard et al., 2000). This suggests that dynamic wobbling of bicelles is not a major influence on the apparent lateral diffusion coefficient under our conditions, but would become significant at lower  $q$  values.

The perforated lamellae model raises another issue, since the toroidal perforations themselves should constitute obstructions to lateral diffusion. Obstructed diffusion is characterized by a crossover from normal diffusion (diffusion distance scales as  $t^{1/2}$ ) at short diffusion times to anomalous diffusion (diffusion distance does not scale as  $t^{1/2}$ ) at longer diffusion times. The degree of obstruction depends most critically on the surface area occupied by the obstructions relative to the percolation threshold above which diffusion can occur only over short distances, but also depends on the size of the diffusant relative to the obstructions and on their geometry (Saxton, 1989, 1993, 1994, 1999). Here we observe only normal diffusion of DMPE-PEG 2000 over a range of diffusion times from 200 to 600 ms. The diffusant DMPE-PEG 2000 may be assumed to be far smaller than any toroidal perforation. The size of an individual perforation, however, is uncertain, so that the surface area occupied by such obstructions for a given value of  $q = \text{DMPC/DHPC}$  is indeterminate. Nevertheless, there should be a dependence of obstructed area on  $q$ . Thus it would be useful to examine lateral diffusion coefficients of DMPE-PEG 2000 in bicelles over a range of  $q$  values and at both shorter and longer diffusion times.

## Prospects for PFG NMR lateral diffusion measurements in bicelles

Our results demonstrate the feasibility of measuring lateral diffusion of DMPE-PEG 2000 in bicelles using STE PFG  $^1\text{H}$  NMR. This feasibility is due in large part to the fact that the PEG-lipid headgroup exhibits a relatively narrow  $^1\text{H}$  NMR resonance line as a consequence of the rapid essentially isotropic internal motion of the PEG group even when anchored to the surface of a magnetically aligned bicelle. This yields an optimal combination of high sensitivity due to proton detection, long gradient encoding period due to long  $T_2$ , and long diffusion time due to long  $T_1$ . It is of interest to examine how readily the STE PFG NMR technique might be applied to measure lateral diffusion of other membrane-associated molecules using other NMR sensitive nuclei in addition to protons.

As Eq. 1 shows, the intensity decay in the STE PFG NMR experiment is proportional to  $\exp(-\gamma^2 g^2 D \delta^2 [\Delta - \delta/3])$ , where  $\gamma$  is the magnetogyric ratio of a particular NMR observable nucleus and  $g$  is the strength of the applied magnetic field gradient. To obtain a comparable intensity decay with some nucleus other than  $^1\text{H}$  requires a commensurate increase in the gradient strength by a factor  $^{\text{H}}\gamma/^\text{X}\gamma$ , as listed in Table 3 for various nuclei of interest. For example, if a gradient strength of  $250 \text{ G cm}^{-1}$  provides adequate intensity decay when measuring the lateral diffusion of DMPE-PEG 2000 via STE PFG  $^1\text{H}$  NMR, then to perform the same measurement using the  $^{31}\text{P}$  NMR resonance under otherwise identical conditions would require a gradient strength higher by a factor of  $\sim 2.5$ . Since this is well within the capabilities of our gradient NMR probe, it would appear that it should be possible to measure lateral diffusion of phospholipids in magnetically aligned bicelles via phosphorus-31 STE PFG NMR. The advantages of  $^{31}\text{P}$  NMR in this regard lie in the fact that it is generally possible to resolve different phospholipids under such circumstances due to their different isotropic and anisotropic chemical shifts, thus permitting simultaneous lateral diffusion measurements on multiple phospholipid species. Relative to the PEG  $^1\text{H}$  NMR resonances investigated here, the shorter  $^{31}\text{P}$   $T_2$  values of

phospholipids mitigate against the experiment, but this consideration is balanced by the longer  $^{31}\text{P}$   $T_1$  values that permit access to long diffusion times  $\Delta$ .

$^2\text{H}$  NMR is widely used to investigate molecular structure and dynamics of both membrane proteins and lipids in a site-specific and nonperturbing manner. The prospects for deuterium STE PFG NMR diffusion measurements appear, at first blush, to be unpromising since the deuterium's magnetogyric ratio is a factor of 6.5 lower than that of the proton, necessitating the application of commensurately larger amplitude gradient pulses. However, two strategies are available for ameliorating this difficulty. One is to encode multiple-quantum coherences of order  $n$  such that the effective gradient strength becomes  $ng$  (Martin et al., 1982). Another involves deuterium stimulated-echo-type PFG NMR experiments incorporating so-called "magic-echo" decoupling to permit use of longer gradient encoding periods (Dvinskikh et al., 2001). Thus, lateral diffusion measurements on deuterium-labeled phospholipids and other amphiphiles appear feasible using deuterium stimulated-echo-type experiments in bicelles.

Fluorine-containing drugs are an important pharmaceutical subclass and many such drugs are lipophilic and associate with membranes (Park et al., 2001; Ismail, 2002). Fluorine's high magnetogyric ratio and low abundance in the absence of specific labeling make fluorine-19 STE PFG NMR an apparently attractive option for measuring lateral diffusion of such drugs in bicelles. The major difficulty with  $^{19}\text{F}$  NMR in an anisotropic medium such as bicelles is the expected large residual dipolar coupling, which limits the length of the gradient encoding period. The "magic echoes" mentioned above should prove remedial in this instance, since they can be used to refocus either quadrupolar or dipolar couplings.

Finally, some comparison of bicelles as a medium for NMR-based lateral diffusion measurements with other such media seems warranted. Relative to supported lipid bilayers such as those used for EXSY NMR diffusion measurements (Fenske and Jarrell, 1991; Picard et al., 1998), bicelles offer enormous signal/noise advantages while avoiding complications due to differences in magnetic susceptibility and hydration at the inner versus the outer monolayer of the supported bilayer. Relative to macroscopically oriented lipid bilayers such as those used in PFG NMR diffusion measurements (Lindblom and Orädd, 1994; Orädd and Lindblom, 2004), bicelles are less robust due to their higher water content and the need to achieve magnetic alignment through magnetic susceptibility effects. For example, the DMPC/DHPC bicelles examined here align only above  $30^\circ\text{C}$  and are unstable above  $50^\circ\text{C}$ . However, altering the long chain phosphatidylcholine to dimyristelaidoyl phosphatidylcholine permits bicelle alignment at temperatures as low as  $5^\circ\text{C}$  (R. S. Prosser, University of Toronto, personal communication). Thus, bicelles appear to retain most of the advantages and avoid most of the disadvantages of other model membrane systems for NMR-based lateral diffusion measurements.

**TABLE 3** comparison of various nuclei for STE PFG NMR lateral diffusion measurements

Nucleus	Magnetogyric ratio $^\text{X}\gamma/10^7 \text{ rad T}^{-1} \text{ s}^{-1}$ *	Relative gradient strength $^{\text{H}}\gamma/^\text{X}\gamma = ^\text{X}g/^\text{H}g^\dagger$
$^1\text{H}$	26.7519	1.0
$^{19}\text{F}$	25.181	1.062
$^{31}\text{P}$	10.841	2.468
$^{13}\text{C}$	6.7283	3.976
$^2\text{H}$	4.1066	6.514

\*Harris (1983).

†Relative gradient strength to achieve identical intensity decay in STE PFG NMR diffusion measurement assuming identical diffusion coefficient, diffusion time, and relaxation times.

Recently, a new PFG NMR lateral diffusion measurement technique has been introduced by Gawrisch and co-workers (Gaede and Gawrisch, 2004, and references therein) in which magic angle spinning (MAS) is imposed to narrow proton resonance lines, in combination with pulsed field gradients to produce sensitivity to diffusion. Although such combined PFG-MAS NMR probes are not yet widely available, PFG NMR probes for solution applications, however, are available, albeit with gradient strengths limited to  $\sim 60 \text{ G cm}^{-1}$ . Such gradient strengths are sufficient, nevertheless, for characterizing equilibrium interactions of small fast diffusing molecules, such as drugs, with lipid bilayers in the form of magnetically aligned bicelles, and for measuring their lateral diffusion within the lipid bilayer.

This research was supported by a grant from the Natural Science and Engineering Research Council of Canada.

## REFERENCES

- Almeida, P. F. F., and W. L. C. Vaz. 1995. Lateral diffusion in membranes. In *Handbook of Biological Physics*. R. Lipovsky and E. Sackmann, editors. Elsevier, Amsterdam, The Netherlands. 305–357.
- Almeida, P. F. F., W. L. C. Vaz, and T. E. Thompson. 1992a. Lateral diffusion in the liquid phases of dimyristoylphosphatidylcholine/cholesterol lipid bilayers: a free volume analysis. *Biochemistry*. 31:6739–6747.
- Almeida, P. F. F., W. L. C. Vaz, and T. E. Thompson. 1992b. Lateral diffusion and percolation in two-phase, two component lipid bilayers. Topology of the solid-phase domains in-plane and across the lipid bilayer. *Biochemistry*. 31:7198–7210.
- Andersson, A., and L. Mäler. 2003. Motilin-bicelle interactions: membrane position and translational diffusion. *FEBS Lett.* 545:139–143.
- Arnold, A., T. Labrot, R. Otle, and E. J. Dufourc. 2002. Cation modulation of bicelle size and magnetic alignment as revealed by solid-state NMR and electron microscopy. *Biophys. J.* 83:2667–2680.
- Bolze, J., T. Fujisawa, T. Naga, K. Norisada, H. Saito, and A. Naito. 2000. Small angle X-ray scattering and  $^{31}\text{P}$  NMR studies on the phase behavior of phospholipid bilayered micelles. *Chem. Phys. Lett.* 329:215–220.
- Callaghan, P. T., and O. Soderman. 1983. Examination of the lamellar phase of aerosol OT/water using pulsed field gradient nuclear magnetic resonance. *J. Phys. Chem.* 87:1737–1744.
- Chung, J., and J. H. Prestegard. 1993. Characterization of field-ordered aqueous liquid crystals by NMR diffusion measurements. *J. Phys. Chem.* 97:9837–9843.
- Cross, K. J., K. T. Holmes, C. E. Mountford, and P. E. Wright. 1984. Assignment of acyl chain resonances from membranes of mammalian cells by two-dimensional NMR methods. *Biochemistry*. 23:5895–5897.
- Crowell, K. J., and P. M. Macdonald. 1999. Surface charge response of the phosphatidylcholine head group in bilayered micelles from phosphorus and deuterium NMR. *Biochim. Biophys. Acta.* 1416:21–30.
- Crowell, K. J., and P. M. Macdonald. 2001. Europium III binding and the reorientation of magnetically aligned bicelles: insights from deuterium NMR spectroscopy. *Biophys. J.* 81:255–265.
- de Gennes, P. G. 1980. Conformation of polymers attached to an interface. *Macromolecules*. 13:1069–1075.
- Du, H., P. Chandaroy, and S. W. Hui. 1997. Grafted poly-(ethylene glycol) on lipid surfaces inhibits protein adsorption and cell adhesion. *Biochim. Biophys. Acta.* 1326:236–248.
- Dvinskikh, S. V., I. Furó, D. Sandström, A. Maliniak, and H. Zimmermann. 2001. Deuterium stimulated-echo-type experiments for measuring diffusion: application to a liquid crystal. *J. Magn. Reson.* 153:83–91.
- Fauth, J.-M., A. Schweiger, L. Braunschweiler, J. Forrer, and R. R. Ernst. 1986. Elimination of unwanted echoes and reduction of dead time in three-pulse electron spin-echo spectroscopy. *J. Magn. Reson.* 66:74–85.
- Fenske, D. B., and H. C. Jarrell. 1991. Phosphorus-31 two-dimensional solid-state NMR: application to model membrane and biological systems. *Biophys. J.* 59:55–69.
- Finer, E. G., A. G. Flook, and H. Hauser. 1972. Mechanism of sonication of aqueous egg yolk lecithin dispersions and nature of the resultant particles. *Biochim. Biophys. Acta.* 260:49–58.
- Flory, P. 1971. *Principles of Polymer Chemistry*. Cornell University Press, Ithaca, NY.
- Gaede, H. C., and K. Gawrisch. 2004. Multi-dimensional pulsed field gradient magic angle spinning NMR experiments on membranes. *Magn. Reson. Chem.* 42:115–122.
- Gaemers, S., and A. Bax. 2001. Morphology of three lyotropic liquid crystalline biological NMR media studied by translational diffusion anisotropy. *J. Am. Chem. Soc.* 123:12343–12352.
- Gibbs, S. J., and C. S. Johnson. 1991. A PFG NMR experiment for accurate diffusion and flow studies in the presence of eddy currents. *J. Magn. Reson.* 93:395–402.
- Glover, K. J., J. A. Whiles, G. Wu, N.-J. Yu, R. Deems, J. O. Struppe, R. E. Stark, and R. R. Vold. 2001. Structural evaluation of phospholipid bicelles for solution-state studies of membrane associated biomolecules. *Biophys. J.* 81:2163–2171.
- Harris, R. K. 1983. *Nuclear Magnetic Resonance Spectroscopy: A Physicochemical View*. Pitman Books, London.
- Hristova, K., and D. Needham. 1995. Phase behavior of lipid-polymer—lipid mixture in aqueous medium. *Macromolecules*. 28:991–1002.
- Ismail, F. M. D. 2002. Important fluorinated drugs in experimental and clinical use. *J. Fluor. Chem.* 118:27–33.
- Jeener, J., B. H. Meier, P. Bachmann, and R. R. Ernst. 1979. Investigation of exchange processes by two-dimensional NMR spectroscopy. *J. Chem. Phys.* 71:4546–4553.
- Johnson, M. E., D. A. Berk, D. Blankschtein, D. E. Golan, R. K. Jain, and R. S. Langer. 1996. Lateral diffusion of small compounds in human stratum corneum and model lipid bilayer systems. *Biophys. J.* 71:2656–2668.
- Jovin, T. M., and W. L. C. Vaz. 1989. Rotational and translational diffusion in membranes measured by fluorescence and phosphorescence methods. *Methods Enzymol.* 172:471–513.
- Kärger, J., H. Pfeifer, and W. Heink. 1988. Principles and applications of self-diffusion measurements by nuclear magnetic resonance. *Adv. Magn. Opt. Reson.* 12:1–89.
- King, V., M. Parker, and K. P. Howard. 2000. Pegylation of magnetically oriented lipid bilayers. *J. Magn. Reson.* 142:177–182.
- Kuo, A.-L., and C. G. Wade. 1979. Lipid lateral diffusion by pulsed nuclear magnetic resonance. *Biochemistry*. 18:2300–2308.
- Lasic, D. D., and D. Needham. 1995. The “stealth” liposome: a prototypical biomaterial. *Chem. Rev.* 95:2601–2628.
- Lindblom, G., and G. Orädd. 1994. NMR studies of translational diffusion in lyotropic liquid crystals and lipid membranes. *Prog. Nucl. Magn. Res. Sp.* 26:483–515.
- Lindblom, G., and L. Rilfors. 1989. Cubic phases and isotropic structures formed by membrane lipids—possible biological relevance. *Biochim. Biophys. Acta.* 988:221–256.
- Liu, C., A. Paprica, and N. O. Petersen. 1997. Effects of size of macrocyclic polyamides on their rate of diffusion in model membranes. *Biophys. J.* 73:2580–2587.
- Losonczi, J. A., and J. H. Prestegard. 1998. Improved dilute bicelle solutions for high-resolution NMR of biological macromolecules. *J. Biomol. NMR.* 12:447–451.
- Marassi, F. M. 2002. NMR of peptides and proteins in oriented membranes. *Concept. Magn. Reson.* 14:212–224.

- Marsh, D., R. Bartucci, and L. Sportelli. 2003. Lipid membranes with grafted polymers: physicochemical aspects. *Biochim. Biophys. Acta*. 1615:33–59.
- Martin, J. F., L. S. Selwyn, R. R. Vold, and R. L. Vold. 1982. The determination of translational diffusion coefficients in liquid crystals from pulsed field gradient double-quantum spin echo decays. *J. Chem. Phys.* 76:2632–2634.
- Meyerhoffer, S. M., T. J. Wenzel, and L. B. McGown. 1992. Lanthanide shift NMR studies of bile salt aggregates. *J. Phys. Chem.* 96:1961–1967.
- Mills, R. 1973. Self-diffusion in normal and heavy water in the range 1–45°. *J. Phys. Chem.* 77:685–688.
- Mukidjam, E., S. Barnes, and G. A. Elgavish. 1986. NMR studies of the binding of sodium and calcium ions to the bile salts glycocholate and taurocholate in dilute solution as probed by the paramagnetic lanthanide dysprosium. *J. Am. Chem. Soc.* 108:7082–7089.
- Nieh, M.-P., C. J. Ginka, S. Krueger, R. S. Prosser, and J. Katsaras. 2001. SANS study of the structural phases of magnetically alignable lanthanide-doped phospholipid mixtures. *Langmuir*. 17:2629–2638.
- Nieh, M.-P., C. J. Ginka, S. Krueger, R. S. Prosser, and J. Katsaras. 2002. SANS study of the effect of lanthanide ions and charged lipids on the morphology of phospholipid mixtures. *Biophys. J.* 82:2487–2498.
- Nyström, B., H. Walderhaug, and F. K. Hansen. 1993. Dynamic crossover effects observed in solutions of a hydrophobically associating water-soluble polymer. *J. Phys. Chem.* 97:7743–7752.
- Opella, S. J., F. M. Marassi, J. J. Gesell, A. P. Valente, Y. Kim, M. Oblatt-Montal, and M. Montal. 1999. Structure of the M2 channel-lining segments from nicotinic acetylcholine and NMDA receptors by NMR spectroscopy. *Nat. Struct. Biol.* 6:374–379.
- Orädd, G., and G. Lindblom. 2004. Lateral diffusion studied by pulsed field gradient NMR on oriented lipid membranes. *Magn. Reson. Chem.* 42:123–131.
- Ottinger, M., and A. Bax. 1998. Characterization of magnetically oriented phospholipid micelles for measurement of dipolar couplings in macromolecules. *J. Biomol. NMR*. 12:361–372.
- Park, B. K., N. R. Kitteringham, and P. M. O'Neill. 2001. Metabolism of fluorine containing drugs. *Annu. Rev. Pharmacol. Toxicol.* 41:443–470.
- Picard, F., M.-J. Paquet, E. Dufourc, and M. Auger. 1998. Measurement of the lateral diffusion of dipalmitoylphosphatidylcholine on silica beads in the absence and presence of melittin: a  $^{31}\text{P}$  two-dimensional exchange solid-state NMR study. *Biophys. J.* 74:857–868.
- Picard, F., M.-J. Paquet, J. Levesque, A. Bélanger, and M. Auger. 1999.  $^{31}\text{P}$  NMR first spectral moment study of the partial magnetic orientation of phospholipid membranes. *Biophys. J.* 77:888–902.
- Price, W. S. 1997. Pulse-field gradient nuclear magnetic resonance as a tool for studying translational diffusion: Part 1. Basic theory. *Concept. Magn. Reson.* 9:299–336.
- Price, W. S. 1998. Pulse-field gradient nuclear magnetic resonance as a tool for studying translational diffusion: Part 2. Experimental aspects. *Concept. Magn. Reson.* 10:197–237.
- Raffard, G., S. Steinbruckner, A. Arnold, J. H. Davies, and E. J. Dufourc. 2000. Temperature-composition diagram of dimyristoylphosphatidylcholine—dicaproylphosphatidylcholine “bicelles” self-orienting in the magnetic field. A solid state  $^2\text{H}$  and  $^{31}\text{P}$  NMR study. *Langmuir*. 16:7655–7662.
- Ram, P., and J. H. Prestegard. 1988. Magnetic field induced ordering of bile salt/phospholipid micelles: new media for NMR structural investigations. *Biochim. Biophys. Acta*. 940:289–294.
- Rowe, B. A., and S. L. Neal. 2003. Fluorescence probe study of bicelle structure as a function of temperature: developing a practical bicelle structure model. *Langmuir*. 19:2039–2048.
- Saffman, P. G., and M. Delbrück. 1975. Brownian motion in biological membranes. *Proc. Natl. Acad. Sci. USA*. 72:3111–3113.
- Sanders, C. R., B. J. Hare, K. P. Howard, and J. H. Prestegard. 1994. Magnetically-oriented phospholipid micelles as a tool for the study of membrane-associated molecules. *Prog. Nucl. Magn. Res. Sp.* 26:421–444.
- Sanders, C. R., and J. H. Prestegard. 1990. Magnetically orientable phospholipid bilayers containing small amounts of a bile salt analogue, CHAPSO. *Biophys. J.* 58:447–460.
- Sanders, C. R., and R. S. Prosser. 1998. Bicelles: a model system for all seasons? *Structure*. 16:1227–1234.
- Sanders, C. R., and J. P. Schwonek. 1992. Characterization of magnetically orientable bilayers in mixtures of dihexanoylphosphatidylcholine and dimyristoylphosphatidylcholine by solid-state NMR. *Biochemistry*. 31:8898–8905.
- Saxton, M. J. 1989. Lateral diffusion in an archipelago. Distance dependence of the diffusion coefficient. *Biophys. J.* 56:615–622.
- Saxton, M. J. 1993. Lateral diffusion in an archipelago. Dependence on tracer size. *Biophys. J.* 64:1053–1062.
- Saxton, M. J. 1994. Anomalous diffusion due to obstacles: a Monte Carlo study. *Biophys. J.* 66:394–401.
- Saxton, M. J. 1999. Lateral diffusion of lipids and proteins. *Curr. Top. Membr.* 48:229–282.
- Stejskal, E. O., and J. E. Tanner. 1965. Spin diffusion measurements - spin echoes in presence of a time-dependent field gradient. *J. Chem. Phys.* 42:288–295.
- Stilbs, P. 1987. Fourier transform pulse-gradient spin-echo studies of molecular diffusion. *Prog. Nucl. Magn. Res. Sp.* 19:1–45.
- Struppe, J., and R. R. Vold. 1998. Dilute bicelle solutions for structural NMR work. *J. Magn. Reson.* 135:541–546.
- Tamm, L. K. 1991. Membrane insertion and lateral mobility of synthetic amphiphilic signal peptides in lipid model membranes. *Biochim. Biophys. Acta*. 1071:123–148.
- Tanner, J. E. 1970. Use of the stimulated echo in NMR diffusion studies. *J. Chem. Phys.* 52:2523–2526.
- Tocanne, J.-F., L. Dupou-Cézanne, and A. Lopez. 1994. Lateral diffusion of lipids in model and natural membranes. *Prog. Lipid Res.* 33:203–237.
- Vaz, W. L. C., F. Goodsaid-Zaluondo, and K. Jacobson. 1984. Lateral diffusion of lipids and proteins in bilayer membranes. *FEBS Lett.* 174:199–207.
- Vaz, W. L. C., M. Criado, V. M. C. Madeira, G. Schoellmann, and T. M. Jovin. 1982. Size dependence of the translational diffusion of large integral membrane proteins in liquid-crystalline phase lipid bilayers. A study using fluorescence recovery after photobleaching. *Biochemistry*. 21:5608–5612.
- Vaz, W. L. C., R. M. Clegg, and D. Hallmann. 1985. Translational diffusion of lipids in liquid crystalline phase phosphatidylcholine multilayers. A comparison of experiment with theory. *Biochemistry*. 24:781–786.
- Vold, R. R., and R. S. Prosser. 1996. Magnetically oriented phospholipid bilayered micelles for structural studies of polypeptides. Does the ideal bicelle exist? *J. Magn. Reson. B*. 113:267–271.
- Wästerby, P., G. Orädd, and G. Lindblom. 2002. Anisotropic water diffusion in macroscopically oriented lipid bilayers studied by pulsed magnetic field gradient NMR. *J. Magn. Reson.* 157:156–159.